JOURNAL OF MATERIALS SCIENCE 5 (1970) 187–197

The Temperature-Dependence of the Strength of Polycrystalline MgO

A. G. EVANS, D. GILLING, R. W. DAVIDGE
Materials Development Division, AERE, Harwell, Didcot, Berks, UK

The temperature-dependence of the strength of a range of polycrystalline magnesias has been studied. Fracture occurs either by the extension of inherent flaws or is initiated by plastic flow. It has been possible to give a quantitative account of the effects of temperature, grain-size, porosity and surface condition on the strength of polycrystalline magnesia.

1. Introduction

There have been many attempts to explain the brittle fracture of polycrystalline oxides but these are mostly empirical in nature and not of general applicability. This paper presents a general approach to strength which can, in principle, be applied to any material at temperatures below that at which significant ductility is obtained. The approach is demonstrated by reference to the temperature-dependence of the fracture strength of a range of magnesias with various grain-sizes and porosities.

It is recognised that fracture can originate either from flaws present prior to testing or from flaws produced by plastic deformation during testing. In the former case the fracture strength (σ_f) is given by a modified Griffith equation:

$$\sigma_f = \left(\frac{2E\gamma_i}{\pi C} \right)^{\frac{1}{2}}, \qquad (1)$$

where E is Young's modulus, γ_i an effective surface energy for fracture-initiation and C a flaw-size. In the latter case flaws are nucleated by plastic processes such as dislocation pile-ups or grain-boundary sliding. Hence, it may be the stress needed to nucleate the flaw or the stress needed to propagate it that is the controlling factor. One requires, therefore, estimates of the stresses needed to propagate existing flaws, to nucleate fresh flaws and to propagate fresh flaws. A comparison of these stresses will indicate the controlling mechanism.

Experimentally, one needs to determine: the effective surface energy for fracture-initiation, the size of existing flaws, and the stresses at which new flaws are created. The flaw nucleation stress is related to the flow stress for primary slip (σ_0) [1] or the macroscopic flow stress (σ_c) [2].

An earlier study [1] showed that the room temperature fracture stress of fully dense MgO is sensitive to the surface condition, the grain-size and the dislocation flow stress. In the chemically polished condition fracture is found to be dislocation-initiated, and is consistent with the stress to initiate a crack according to the Stroh model [3]. The fracture stress is given by:

$$\sigma_f = \sigma_0 + k_s G^{-\frac{1}{2}}, \qquad (2)$$

where k_s is a constant that depends on the energy for crack-initiation and G is the grain-size: σ_0 is independent of grain-size. The temperature-dependence of the strength of a similar material, in the chemically polished condition, has been studied by Day and Stokes [4]. Between 600 and ~1400° C the fracture stress is found to decrease with an increase in temperature in a manner similar to the single crystal flow stress. They suggested, therefore, that fracture in this temperature range is dislocation-initiated, which is consistent with our room temperature observations. In the as-machined condition, at room temperature, the fracture mechanism is different and fracture occurs by the extension of the flaws produced by machining. The fracture stress is given quantitatively by equation 1. The temperature-dependence of the strength of as-machined material should differ, therefore, from that for chemically polished material.

Four magnesias are used in this study: the fully dense material used previously with grain-

sizes of 25 or 150 μm, and two porous materials: 97% dense, grain-size 25 μm, and, 85% dense, grain-size 20 μm. The temperature-dependence of the fracture stress from 20 to 1700° C is measured for specimens with either machined or polished surfaces. These stresses are compared with the stress needed to propagate existing flaws, the primary slip stress, σ_0, and the macroscopic flow stress, σ_c. The temperature-dependence of σ_0 is obtained from the flow stress of single crystal MgO with a room temperature flow stress similar to that of the polycrystals. The macroscopic flow stress is determined from compression tests on the polycrystalline material. Microscopy observations indicate the nature of both the pre-existing flaws and the flaws formed during deformation.

In this way it has been possible to give a comprehensive and quantitative explanation of the effects of grain-size, pore-size, flow stress, temperature and surface condition on the strength of polycrystalline magnesia.

2. Experimental

The fully dense material was prepared as described by Miles *et al* [5]. The as-pressed discs were annealed in argon for 1 h at 1750 and 1950°C to give grain-sizes of 25 μm and 150 μm respectively. The porous materials were prepared from powder supplied by Kanto Ltd. One was hot-pressed in air in a graphite die at 2000 psi,* at 1800° C for $\frac{1}{2}$ h, and the other cold-pressed at 10000 psi and sintered at 1600° C for 12 h. The former material was 97% dense with a grain-size 25 μm and the latter ~85% dense with a grain-size 20 μm.

The fracture stresses were determined in three-point bending using specimens with dimensions 22 × 4 × 3 mm and a knife edge span of 18 mm. Tests up to 1500° C were conducted in air in a small SiC furnace and those at higher temperatures in a molybdenum furnace in an argon atmosphere. At least four specimens were tested at each temperature.

γ_i values were obtained, also from three-point bend tests, by inserting the stress, σ, to extend sharp single edge cracks of length C, into the following equation:

$$\sigma = \frac{1}{Y}\left(\frac{2E\gamma_i}{C}\right)^{\frac{1}{2}} \quad (3)$$

where Y is a numerical factor that depends upon the geometry of the system [6]. The sharp edge cracks were introduced by driving a wedge into a shallow notch in a controlled manner [7]. However, it has been found that equation 3 applies approximately to machined notches, where C is the length of the notch [1], because machining introduces sharp cracks along the root of the notch. Most experiments were thus conducted, for convenience, on bars with machined notches, with a smaller number of confirmatory experiments on bars with long sharp cracks. Some experiments were also conducted on notched bars which were annealed at various temperatures for 20 min – the time that a specimen is normally held at temperature prior to testing – and then tested at room temperature. This would indicate whether changes in γ_i are due to irreversible structural alterations at the test temperature.

The temperature-dependence of the primary dislocation flow stress, σ_0, was measured on a single crystal that had a room temperature flow stress similar to that of the fully dense polycrystals, 180 MN m^{-2}. The flow stress was determined in bending using a ⟨100⟩ stress axis. The specimens were annealed at 1800° C after cleavage and sprinkled with carborundum powder prior to testing [8].

The macroscopic flow stress of all the polycrystals was determined from the compressive yield stress using compression specimens with dimensions 8 × 4 × 3 mm.

3. Results

3.1. The Temperature-Dependence of the Fracture Stress

The fracture stresses of the fully dense material between room temperature and 1700° C are shown in fig. 1a. For polished material σ_f falls monotonically with increasing temperature to an approximately constant value at 1200° C (25 μm grain-size) or 1400° C (150 μm grain-size). The fine-grained material is the stronger at all temperatures. At the lower temperatures σ_f is lower for machined material than for polished material, whereas, at higher temperatures, the curves for machined and polished materials coincide. All fractures are brittle, i.e. there is no deviation from linearity in the load-deflection curves, below 1500° C. Above this temperature, the 25 μm grain-size material shows some plasticity but the plastic strain never exceeds 2%.

The fracture stresses of the porous materials are shown in fig. 1b. The as-machined, hot-

*1 psi = 6894.76 N m^{-2}

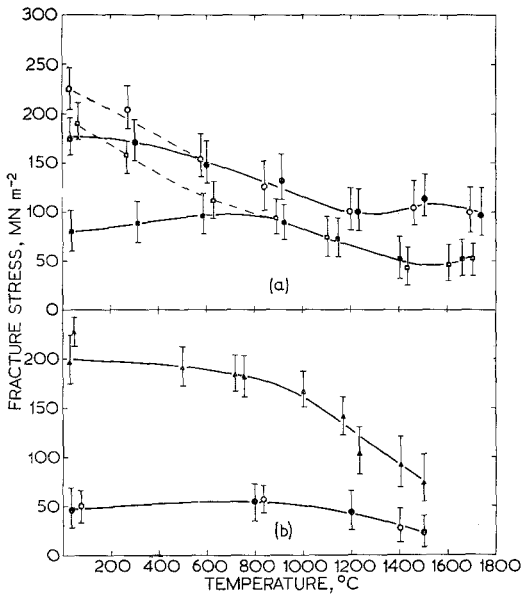

Figure 1 The temperature-dependence of the fracture stress: (a) fully dense material; $G = 25\mu$m, ○, chemically polished, ●, as-machined; $G = 150\mu$m, □, chemically polished, ■, as-machined. (b) hot-pressed; ▲, mechanically and chemically polished, △, as-machined; cold-pressed, ○, mechanically polished, ●, as-machined.

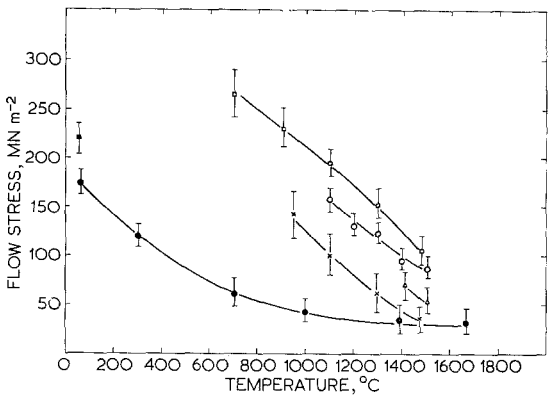

Figure 2 Temperature-dependence of the macroscopic flow stress and the flow stress for primary slip. Macroscopic flow stress σ_c, ○, fully dense, $G = 25\mu$m, △, fully dense, $G = 150\mu$m, □, porous hot-pressed, $G = 25\mu$m, X, porous, cold-pressed, $G = 20\mu$m. Flow stress for primary slip, σ_o, ●, fully dense, ■, porous, hot-pressed.

pressed material is stronger at room temperature than the fully dense material of similar grain-size and compares well with results obtained on similar material by Vasilos *et al* [9]. The fracture stress is virtually temperature-independent up to ~600° C and then decreases with increase in temperature. The rate of decrease above 1200° C is more rapid than in the fully dense material, so that the strengths are similar at ~1400° C. Removing the machining flaws by a combination of mechanical and chemical polishing, has a similar effect to that encountered in the fully dense material. Thus, the strength is increased at low temperatures, where the fracture stress of the as-machined material is temperature-independent, but polishing has no effect at higher temperatures. The strength of the cold-pressed and sintered material is very much lower. It is temperature-independent up to ~1100° C, and then decreases with an increase in temperature. In contrast to the other materials the removal of the machining flaws has no significant effect on the strength.

3.2. The Temperature-Dependence of the Flow Stresses

The flow stress of the single crystal MgO – twice the critical resolved shear stress – is shown in fig. 2. This gives an approximate temperature-dependence of σ_o for the fully dense material. A value of σ_o was obtained in the hot-pressed, porous material at room temperature, using the indentation wing technique [1, 8]. It is found to be 220 MN m^{-2}. This is larger than the value obtained in the fully dense material, which implies that there is a larger concentration of impurity within the grains. Unfortunately, it has not been possible to apply the indentation technique successfully to the porous, cold-pressed material, so a value of σ_o for this material is not available.

The macroscopic flow stresses (σ_c) of the various polycrystalline materials are also shown in fig. 2. The porous hot-pressed, material exhibits plastic flow in compression above 700° C, whereas the fully dense materials do not deform plastically below 1100 and 1400° C for the 25 μm and 150 μm grain-size materials respectively (fig. 3). A similar observation has been made by Copley and Pask [10]. The porous, cold-pressed material exhibits ductility above 900° C. σ_c for the porous, hot-pressed material is always higher than that of the fully dense material. This is consistent with the larger value of σ_o, i.e. an increase in the concentration of impurity within grains would increase the secondary as well as the primary slip stress [11]. In the fully dense material, σ_c increases with decrease in grain-size. A similar trend is en-

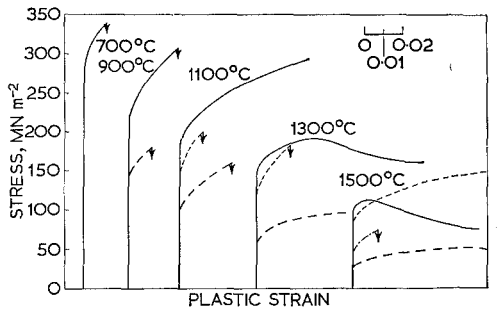

Figure 3 Compressive stress-strain curves as a function of temperature. — porous, hot-pressed; - - - - fully dense, $G = 25\mu m$; ····· fully dense, $G = 150\mu m$; — — — — porous, cold-pressed and sintered.

countered in metals and has been explained by Petch [12]. The porous, cold-pressed material has the lowest σ_c. Since a value of σ_o is not available for this material, it is not clear whether this low σ_c is due to a low impurity level within the grains or to deformation around the pores [13].

Finally, it is interesting to note that work-softening is observed in the porous hot-pressed material above 1300° C and that limited grain-boundary migration accompanies deformation in the fully dense, fine-grained, material above 1400° C.

3.3. The Effective Surface Energy for Fracture Initiation γ_i

The γ_i values obtained for half-way-through single edge notches and sharp cracks are shown in fig. 4. These are valid according to the ASTM specifications [6] up to 1300° C. Above this temperature, the fracture stress of the bars is $> 0.4\ \sigma_o$. The plastic zones around the notches must therefore be relatively large, and the values of γ_i obtained may be in error.

The values obtained for sharp cracks are similar at all temperatures to those for notches. Thus, the notched bar experiments give true γ_i values. γ_i is virtually temperature-independent for the fully dense and porous, cold-pressed materials, but decreases slowly with increase in temperature for the porous, hot-pressed material. In the fully dense material there is an increase in γ_i with increase in grain-size (fig. 4a), as observed in pure polycrystalline alumina [14]. γ_i for the 97% dense material is larger than that for the 85% dense material, fig. 4b.

In the fully dense material, γ_i depends on the

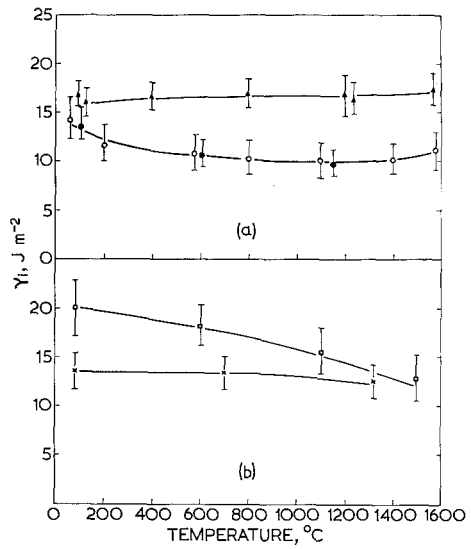

Figure 4 The temperature-dependence of γ_i: (a) fully dense material, $G = 25\mu m$, ○, notched bar, ●, sharp crack; $G = 150\mu m$, △, notched bar, ▲, sharp crack. (b) porous materials, □, porous, hot-pressed, notched bar, X, porous, cold-pressed, sintered, notched bar.

crack length, C, for cracks $< 10G$, e.g. for 20 μm grain-size material, γ_i is reduced to 4 J m^{-2} for $C = 2G$ [1]. In Al_2O_3 and UO_2, however, γ_i is independent of C, at least at room temperature, so the effect is genuinely related to the properties of the material and is peculiar to MgO. Thus, the crack length-dependence of γ_i has been evaluated for the porous materials, to see whether they exhibit a similar effect. In the hot-pressed, porous material a decrease is observed, and γ_i at room temperature is reduced to $\sim$5 J m^{-2} for $C = 2G$. In the cold-pressed and sintered material, the pre-existing flaws are $> 40G$ in diameter (see section 3.4) and it is not possible, therefore, to insert flaws smaller than this. For flaws $> 40G$ in length, it is found that there is no significant variation of γ_i with crack length.

γ_i values were also obtained at room temperature on specimens pre-annealed for 20 min at elevated temperatures. There is no significant change, for anneals up to 1400° C. This indicates that the flaw geometry is unaffected at these temperatures.

Finally, observations were made of the plastic zone ahead of a sharp crack as the stress was raised. The diameter of the plastic zone increases with increase in stress, as expected. It was also observed, however, that microcracks are created ahead of the main crack at stresses $> 90\%$ of

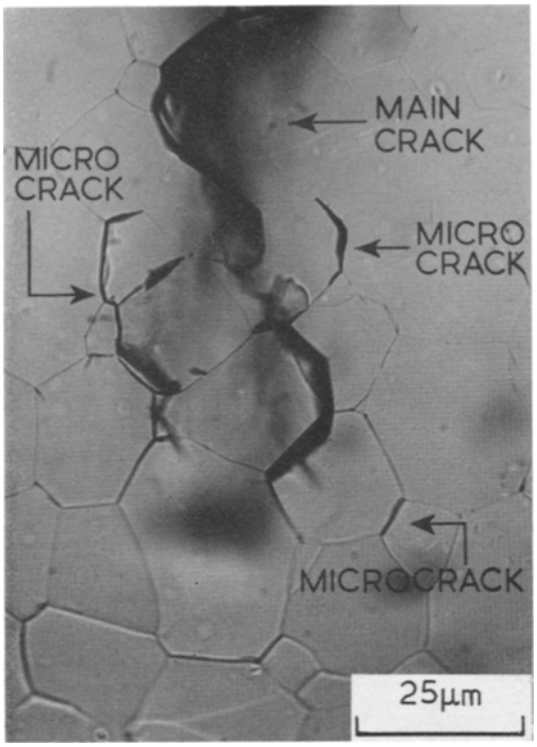

Figure 5 Microcracks ahead of a pre-existing crack at ~90% of the fracture load; transmitted light.

the fracture stress (fig. 5). They were observed regularly for tests above 1000° C but infrequently at lower temperatures. When these microcracks are created, catastrophic fracture presumably occurs when these link up with the main crack. The crack is thus extended prior to catastrophic propagation. In the determinations of γ_i, therefore, the flaw size should be that at the point of catastrophic propagation and not the initial dimensions. The extension is only of the order of a few G, so it is not significant for half-way-through notches. The results in fig. 4 are thus unaffected. The effect is likely to be important for small flaws, however, and may account, at least in part, for the crack length-dependence of γ_i for small crack lengths.

3.4. The Determination of the Flaw Size

In the fully dense material, the largest flaws in the chemically polished condition are grain-boundary grooves of depth $\leqslant 3$ μm; whereas in the as-machined condition, the largest flaws are grain-size cracks and grain pull-outs [1]. In the porous hot-pressed material, the flaws in the polished condition are small pores (fig. 6a). These are generally $\sim 0.1G$ in diameter but can be as large as $\sim 0.2G$, After machining, grain-size cracks and grain pull-outs are again observed. In the cold-pressed and sintered material, pores very much larger than the grain diameter are observed (fig. 6b). The largest of these are $\sim$ 800 μm long. These are thus the largest flaws in both the polished and as-machined conditions.

Under certain conditions, flaws can be created under stress prior to catastrophic failure. Thus, on specimens polished before testing at 1200° C, a large number of grain-size cracks are observed on the tensile face, at stresses $>$ 90% of the fracture stress. The cracks are largely inter-granular in the fully dense material (fig. 7a), whereas a large proportion of transgranular

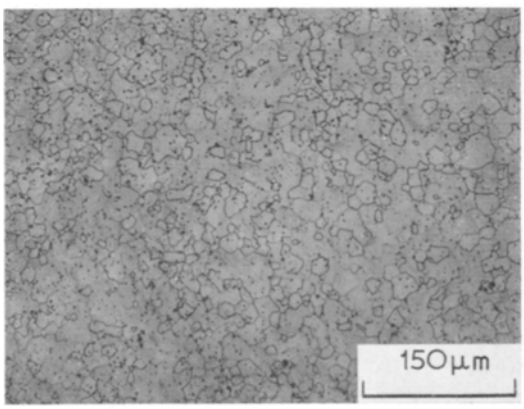

(a)

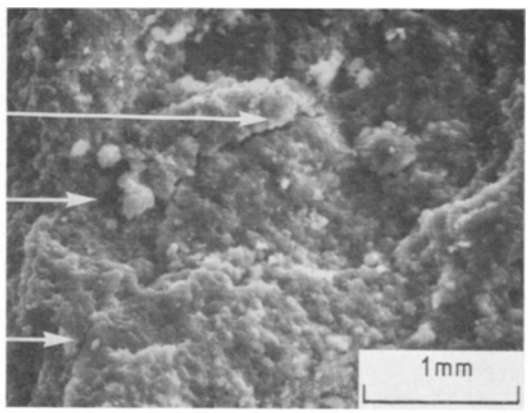

(b)

Figure 6 The size and distribution of pores in: (a) hot-pressed material, optical micrograph; (b) cold-pressed and sintered material, scanning electron fractograph – flaws arrowed.

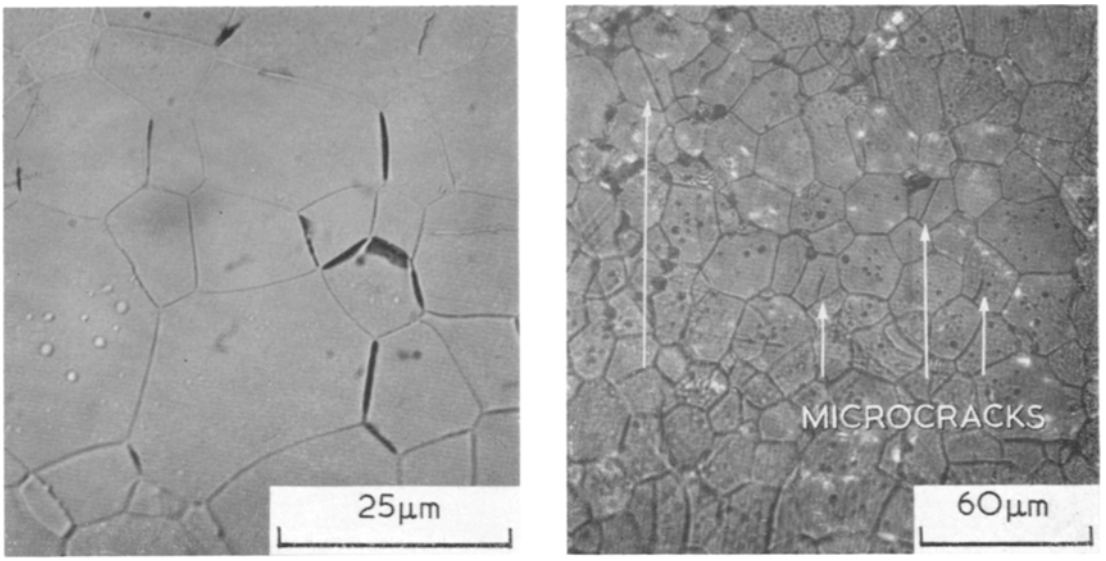

Figure 7 The generation of microcracks at ~90% of fracture stress at 1100° C: (a) fully dense material, transmitted light; (b) hot-pressed, porous material, reflected light.

cracks are observed in the hot-pressed porous material (fig. 7b). The average density of microcracks on a cross-section is about one per twenty grains but the local density, as in fig. 7a for instance, can be very much higher.

3.5. Topography of the Fracture Faces

Fracture faces were examined optically and in the scanning electron microscope to see whether the features of the topography could be related to the observed fracture characteristics. The principal difference between the materials is the varying proportion of transgranular fracture. In the fully dense material, the proportion increases with increase in grain size, from ~ 2% in the finer-grained material (fig. 8a) to ~ 10% in the coarser-grained material, and does not vary significantly with temperature. In the porous,

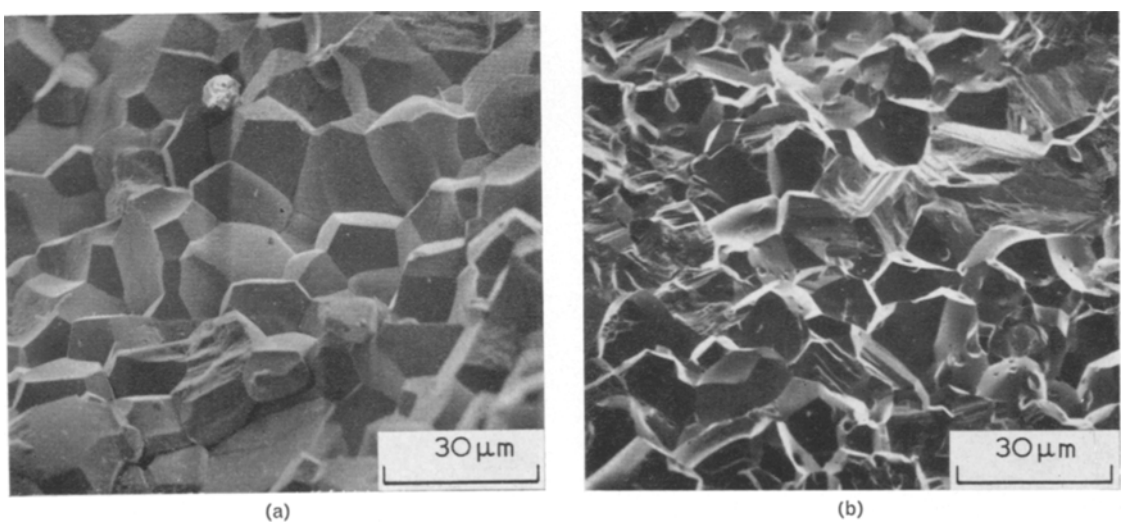

Figure 8 Scanning electron fractographs for room temperature fracture: (a) fully dense, 25 μm grain-size material; (b) porous, hot-pressed material.

hot-pressed material there is very much more transgranular fracture at room temperature, $\sim$ 40% (fig. 8b) but the proportion decreases with increase in temperature, e.g. to $\sim$ 5% at 1400° C. The cold-pressed and sintered material has $\sim$ 5% transgranular fracture at all temperatures.

4. Discussion

4.1. The Effective Surface Energy for Fracture Initiation γ_i

The measured γ_i values are $> \gamma_o$, the thermodynamic surface energy, The difference between γ_i and γ_o can be accounted for largely by a plastic flow contribution, γ_p [15]. The dependence of γ_i on temperature, grain-size and porosity, is discussed, therefore, in terms of their effect on γ_p.

Gilman [16] has shown that γ_p is proportional both to the energy for crack propagation in the absence of plastic flow, γ_o – and hence the mode of fracture – and to a function of Young's modulus divided by the stress needed to move dislocations.

The grain-size-dependence of γ_p has been discussed previously [2]. It is shown that, for a material of given purity, γ_p should increase with an increase in grain-size, which is consistent with the observed grain-size-dependence of γ_i for the fully dense material (fig. 4a). The temperature-dependence of γ_p is more difficult to predict. Both Young's modulus [17] and the stress needed to move dislocations (fig. 2) decrease with increase in temperature. γ_p is expected, therefore, to vary less with temperature than either E or σ_o which is in qualitative agreement with the observed temperature-dependence of γ_i.

The effect of porosity on γ_i depends upon whether fracture is trans- or inter-granular. Pores within grains tend to be spherical so, for transgranular fracture, the pores blunt the crack at various points along its length [18] and give an apparent increase in γ_i. Conversely, pores at grain-boundaries have sharp angles where the boundary and the pore meet [2]. They do not blunt the crack, therefore, but merely reduce the surface area that has to be created by the propagating crack. This effectively reduces γ_o and hence γ_p. It may not be possible to fit the observed porosity-dependence of γ_i into this framework, however, because the purity of the material is variable. Thus, the stress needed to move dislocations and the proportion of transgranular fracture varies in each material. Both affect γ_p, and the variation of γ_i may be related primarily to these effects. It is interesting to note, however, that where the modes of fracture are comparable – in the fully dense and 85% dense materials – porosity has little effect on γ_i (fig. 4b). The significance of this is considered later.

4.2. The Fracture Mechanisms

The stress needed to extend inherent flaws is compared with the measured fracture stress (fig. 9) for each of the four materials and two surface conditions. The inherent flaws comprise grain-boundary grooves, machining flaws of about one grain diameter, or pores; for each material and surface condition it is the lowest flaw extension stress that is important. Two cases can be considered. When the fracture stress and the stress needed to extend the largest flaws are equivalent, the fracture mechanism is identified immediately. When the fracture stress is lower than the inherent flaw extension stress, a plastic deformation-initiated fracture is indicated; here a comparison with the dislocation flow stress and the compressive flow stress is useful. This is clearly a complex analysis and it is convenient to consider the two cases separately.

4.2.1. Fracture Initiated from Inherent Flaws

In fully dense material in the as-machined condition, the flaws are grain-sized cracks and pull-outs. The stress needed to extend these flaws is obtained by inserting γ_i for the appropriate flaw size, and E into equation 1, and is shown in figs. 9a and b.

The flaws in the machined, porous, hot-pressed material are similar to those in fully dense material of a similar grain-size. Since γ_i is larger, however, the stress needed to extend these flaws is larger than in the fully dense material, fig. 9c. Removal of the machining flaws by polishing, leaves the small pores (fig. 6a) as the inherent flaws. The spacing between the pores is small compared to their size, so the stress (σ_p) needed to extend them is given by the following equation [19]:

$$\sigma_p = \left(\frac{\pi E \gamma_i}{2C}\right)^{\frac{1}{2}}. \qquad (4)$$

The initial extension of a pore occurs along the grain-boundary containing it. γ_i for this process is the grain-boundary fracture energy, i.e. $\sim 0.7\ \gamma_o$ [1]. The stress needed to extend the largest pores to a grain dimension is obtained, therefore, by inserting this γ_i value and a value for C of

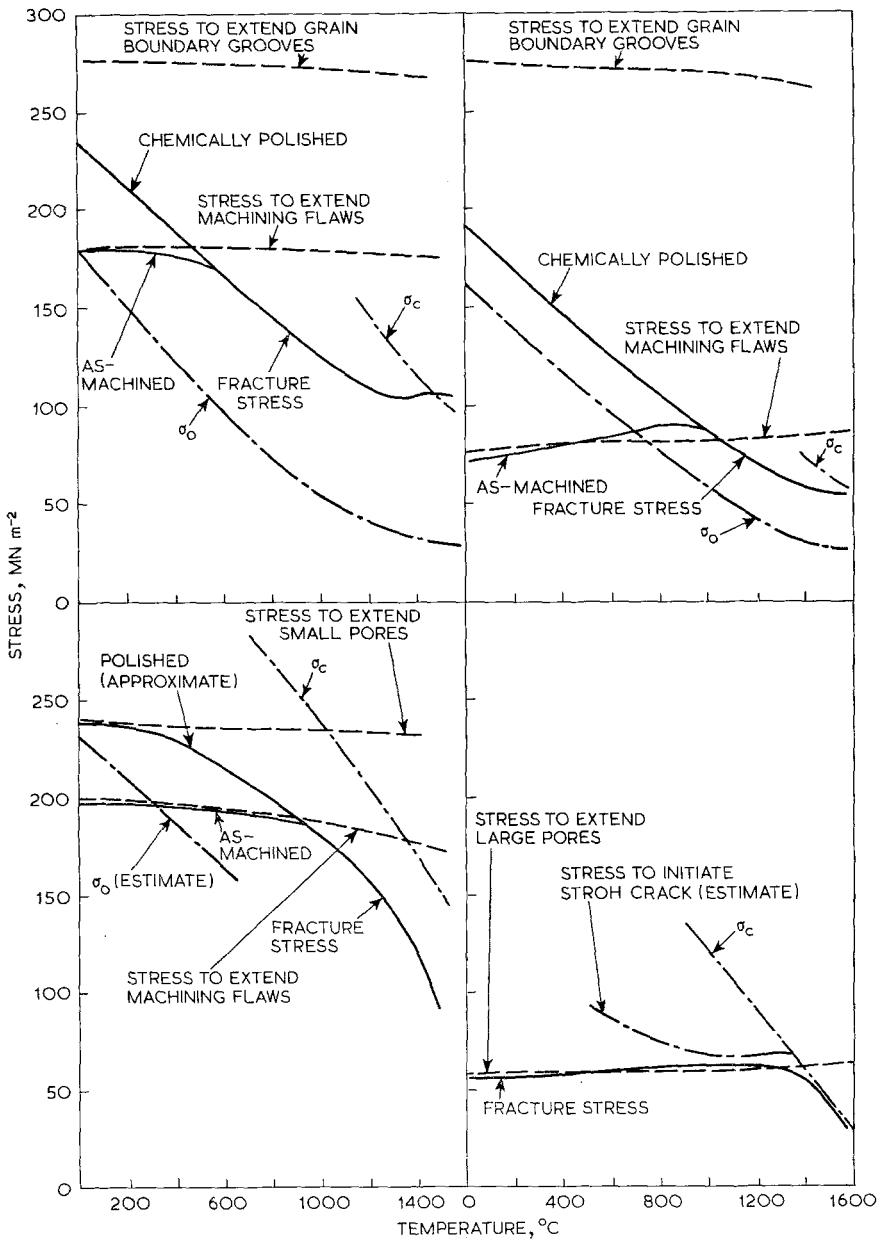

Figure 9 The temperature-dependence of the fracture and flow stresses and the stresses needed to extend pre-existing flaws: (a) fully dense, $G = 25$ μm; (b) fully dense, $G = 150$ μm; (c) porous, hot-pressed; (d) porous, cold-pressed and sintered.

$\sim 0.2G$ into equation 4, fig. 9c. This is larger than the stress needed to extend grain-size cracks given by equation 1, so that the extension of the pore is the controlling process.

Finally, the flaws in the cold-pressed and sintered material are the large pores shown in fig. 6b. The stress needed to extend these pores along the adjacent grain-boundaries, given by equation 4, is ~ 10 MN m^{-2}, i.e. well below the observed fracture stress. Further extension of the flaws is a more complex process and γ_i increases to the measured value given in fig. 4b. The stress needed to propagate the pores to fracture (fig. 9d) is thus given by inserting this value of γ_i and a flaw size of $\sim 40G$ into equation 4.

Thus, it is seen (fig. 9) that fracture occurs by

the extension of the inherent flaws in the following cases: (a) fully dense material, machined surface, 25 μm grain-size: $< 600°$ C; (b) fully dense material, machined surface, 150 μm grain-size: $< 900°$ C; (c) porous hot-pressed material, machined surface: $< 800°$ C; (d) porous hot-pressed material, polished surface: $< 500°$ C; (e) porous cold-pressed and sintered material, machined or polished surface: $<1300°$ C.

4.2.2. Fracture Initiated by Plastic Flow

In the fully dense materials, the fracture stress of the polished specimens is well below the stress needed to extend the inherent flaws – the grain-boundary grooves – at all temperatures, figs. 9a and b. For the machined specimens, the fracture stress is below the grain-sized flaw extension stress at temperatures $> 600°$ C (25 μm grain-size) or $> 900°$ C (150 μm grain-size). In these cases it is concluded that fracture is dislocation-initiated.

The fracture stresses are in excess of σ_0, the flow stress for primary slip, but lower than σ_c the macroscopic flow stress (fig. 9a). Fracture is thus initiated by limited dislocation motion, largely on the primary system. At room temperature, it has been shown that the experimental fracture stresses correspond to the stress needed to initiate Stroh cracks (equation 2), where σ_0 is the flow stress for primary slip in favourably oriented grains [1]. This flow stress is the stress needed to form slip bands so that cracks are only nucleated when a slip band has formed. A similar observation has been made in bicrystals [20]. The nature of the slip band may be determined from the grain-size proportionality factor k_s. The larger k_s is compared with the theoretical value – for nucleation by a pile-up on a single slip plane [21, 22] – the broader the slip band, and the fewer the number of dislocations on each plane within the band [23].

Examination of the current grain-size and temperature effects on fracture strength shows that at temperatures $< 1300°$ C the fracture strength extrapolates to σ_0 at infinite grain-size and that the calculated values of k_s are close to the theoretical values. Fracture, therefore occurs at the stress needed to nucleate cracks by a *narrow* slip band. At temperatures $> 1300°$ C the fracture strengths are larger than expected, but this could be due to an increase in k_s. This may be related to an increase in the ease of cross-slip which results in a broadened slip band. Alternatively grain-boundary migration or increased difficulty in crack propagation could be important.

Since fracture appears to be controlled by the stress needed to nucleate Stroh cracks – at least at temperatures $< 1300°$ C – the cracks must be able to propagate to fracture at a stress lower than the nucleation stress. It is believed that the crack can grow to a grain dimension at the nucleation stress, but it remains to be shown that such cracks can lead to catastrophic fracture. At low temperatures, where the strength of polished specimens is greater than that of machined specimens (which contain grain-sized cracks) the creation of a grain-size crack is clearly the controlling mechanism. But at higher temperatures the fracture stress is lower than that needed to propagate grain-sized cracks. Thus, some linking of cracks to form a flaw large enough for catastrophic fracture is required; the evidence in figs. 5 and 7 gives support to this.

In the porous hot-pressed material the fracture stress above 800° C varies with temperature in a manner similar to that observed in the fully dense material. It also lies between σ_0 and σ_c (fig. 9c). Fracture in this temperature range is likely therefore to be initiated by limited dislocation motion as in the fully dense material. The larger fracture stress in the porous material can be related directly to the larger value of σ_0, so the form of the crack-initiating slip band must be similar in both materials. Above $\sim 1300°$ C, unlike the fully dense material, the strength continues to decrease. It is also noted that this is the temperature where work-softening is first encountered in the compression tests. The two effects may be related.

In the porous, low-density material above 1200° C the fracture stress is lower than the stress needed to extend the pores and similar to the macroscopic flow stress. Fracture is thus initiated by plastic flow. This situation is identical to that encountered in polycrystalline UO_2, containing pores $> G$ in diameter [2]. Fracture, corresponding to the stress needed to initiate Stroh cracks, is not encountered in this material. This implies that the stress needed to extend the pores is always lower than the stress needed to initiate Stroh cracks as depicted in fig. 9d. This may be possible if the stress needed to initiate cracks becomes temperature-independent, as in the fully dense material above $\sim 1200°$ C (fig. 9a). This may occur when secondary slip

partially relieves the stress concentration at grain-boundary pile-ups. Then, although slip occurs in favourably oriented grains throughout the specimen, the initial primary dislocation pile-ups do not initiate sufficient microcracks for fracture to occur. More extensive dislocation motion is required, therefore, to initiate enough cracks for catastrophic fracture.

4.3. The Rôle of Dislocation Motion in Fracture

It is clear from the preceding discussion that dislocation motion exhibits a dual role in the fracture of polycrystalline MgO. At low temperatures it is confined to the vicinity of the pre-existing flaws. It reduces the stress concentration at the tip of the flaws and hence, contributes to γ_i. This is beneficial to strength. At high temperatures, plastic deformation can occur throughout the specimen, in favourably oriented grains, before the stress needed to extend inherent flaws is reached. Microcracks are formed, which lead to fracture. This is deleterious to strength. There must also be an intermediate temperature range where cracks are initiated in the plastic zone ahead of a pre-existing flaw (fig. 5). Here plastic flow both extends pre-existing flaws and increases γ_i, and could be beneficial or deleterious. In this range, fracture occurs at a stress lower than that predicted by inserting the original flaw size into equation 2. The difference becomes significant when the extension, prior to catastrophic propagation, and hence the plastic zone size, is comparable to the dimensions of the pre-existing flaw. The plastic zone size is almost as large as the flaw size in as-machined material at room temperature [1]. This intermediate range could, therefore, commence at quite low temperatures.

4.4. The Effect of Porosity on Fracture

The effect of porosity on strength is complex. The total porosity has little effect on γ_i. Thus when fracture occurs by the extension of pre-existing flaws the fracture stress is related to the effect of the porosity on Young's modulus and the size of the flaw. Porosity invariably reduces Young's modulus, largely through a reduction in load bearing area. The reduction is large, e.g. a 70% reduction for a change in porosity from 0 to 15% [24]. The effect on the fracture stress is smaller, however, because $\sigma \propto E^{\frac{1}{2}}$, e.g. a reduction in stress of $\sim 40\%$ for the above porosity change. The effect of porosity on the flaw-size is more critical. In as-machined material, for instance, if the largest pores are $< G$, the pores do not have a significant effect on the flaw-size. The strength is then only affected through Young's modulus. In this case, an 85% dense material could have a strength as large as $\sim 60\%$ of that for fully dense material of similar grain-size and purity. When the pores are $> G$, however, the pores become the largest flaws and the strength is further reduced by an amount proportional to the square root of the pore-size. Thus, in the cold-pressed and sintered material with pores $\sim 40G$ in diameter, the strength is reduced to $< 30\%$ of that for the fully dense material. Finally, pores, even if $< G$, reduce or nullify the strength increase that can be achieved by polishing the specimen surfaces.

5. Conclusions and Implications

The fracture of polycrystalline MgO is a complex process. The mode of fracture, at a given temperature, depends on grain-size, surface finish, the quantity and size of the pores, and the quantity and distribution of the impurity.

In fully dense material with polished surfaces, fracture is initiated by plastic flow. Up to 1300°C, fracture is consistent with the stress needed to initiate cracks by a pile-up of primary dislocations. The pile-up is in the form of a narrow slip-band. Sufficient microcracks are formed at the initiation stress to enable them to link up and propagate to fracture. Above 1300° C, fracture is complicated by the onset of grain-boundary migration.

The stress needed to initiate cracks by grain-boundary pile-ups can be raised by decreasing the grain-size, increasing the stress needed to move dislocations within grains and increasing the strength of the grain-boundaries. The most effective of these is increasing the stress needed to move dislocations. This is shown clearly by the difference in fracture stress between the 97% dense and fully dense materials in the polished condition. More effective increases may be achieved, for instance, by controlled impurity additions, provided they do not segregate to the grain-boundaries and lower their strength.

When the surfaces are machined, grain-size cracks form at the surface. These reduce the fracture stress at low temperatures. Fracture then occurs by the extension of the surface flaws and the fracture stress is determined by γ_i and the flaw-size, i.e. the grain-size. The smaller the

surface grain-size, the larger is the fracture stress. γ_i appears to be related strongly to the strength of the grain-boundaries in addition to its dependence on the stress needed to move dislocations. The "cleaner" the grain-boundaries, the larger γ_i and thus, the larger the fracture stress.

The effect of porosity on strength is related to the pore-size as well as the total porosity. The total porosity affects strength through a Young's modulus term, whilst the pore-size determines the magnitude of the inherent flaws. Thus, if the material is to be used in the as-machined condition, the pore-size should be $< G$. The pores then have little effect on the flaw-size and affect the strength only through Young's modulus.

In materials where large pores, $\gg G$, are present, the stress needed to extend the pores is less than the stress needed to initiate large numbers of cracks by the Stroh mechanism. Thus, sufficient microcracks to cause fracture are only initiated after extensive dislocation activity. The fracture stress then approximates to the macroscopic flow stress.

Acknowledgements

The authors wish to thank R. A. J. Sambell for providing the fully dense material, J. R. McLaren for the photograph in fig. 8b and Miss G. Tappin for conducting the compression tests.

References

1. A. G. EVANS and R. W. DAVIDGE, *Phil. Mag.* **20** (1969) 373.
2. *Idem, J. Nucl. Matls.* **33** (1969) *in press.*
3. A. N. STROH, *Advances in Physics* **6** (1957) 418.
4. R. B. DAY and R. J. STOKES, *J. Amer. Ceram. Soc.* **49** (1966) 345.
5. G. D. MILES, R. A. J. SAMBELL, J. RUTHERFORD, and G. W. STEPHENSON, *Trans. Br. Ceram. Soc.* **66** (1967) 319.
6. W. F. BROWN and J. E. SRAWLEY, *ASTM*, STP (1967) 410.
7. R. W. DAVIDGE, and G. TAPPIN, *Proc. Br. Ceram. Soc.* **15** (1970) in press.
8. R. W. DAVIDGE, *J. Mater. Sci.* **2** (1967) 339.
9. T. VASILOS, J. B. MITCHELL, and R. M. SPRIGGS, *J. Amer. Ceram. Soc.* **47** (1964) 606.
10. S. M. COPLEY and J. A. PASK, *Mater. Sci. Res.* **3** (1966) 189.
11. A. G. EVANS, *Proc. Br. Ceram. Soc.* **15** (1970) in press.
12. N. J. PETCH, *Prog. Met. Phys.* **5** (1956) 1.
13. G. M. JENKINS, "Proceedings of the International Conference on Structure Solid Mechanics and Engineering Design in Civil Engineering Materials", 1969 (John Wiley, London and New York) to be published.
14. P. L. GUTSHALL and G. R. GROSS, *Eng. Frac. Mech.* **1** (1969) 463.
15. J. CONGLETON, N. J. PETCH, and S. A. SHIELS, *Phil. Mag.* **19** (1969) 795.
16. J. J. GILMAN, "Fracture", edited by B. L. Averbach, D. K. Felbeck, G. T. Hahn and D. A. Thomas (John Wiley, London & New York, 1959) p. 193.
17. D. H. CHUNG, G. R. TERWILLIGER, W. R. CRANDALL, and W. G. LAWRENCE, (1964) U.S. Army Research Report (Durham), Contract No. -DA-31-124-ARO(D-23).
18. E. M. PASSMORE, R. M. SPRIGGS, and T. VASILOS, *J. Amer. Ceram. Soc.* **48** (1965) 1.
19. R. A. SACK, *Proc. Phys. Soc.* **58** (1946) 729.
20. R. C. KU and T. L. JOHNSTON, *Phil. Mag.* **9** (1964) 231.
21. E. SMITH and J. T. BARNBY, *Met. Sci. J.* **1** (1966) 1.
22. P. T. HEALD, *Scripta Met.* **3** (1969) 393.
23. E. SMITH, *Acta Met.* **16** (1968) 313.
24. D. H. CHUNG, *Phil. Mag.* **8** (1963) 833.

Received 12 November and accepted 13 November 1969.